COBEM 2023 27TH INTERNATIONAL CONGRESS OF MECHANICAL ENGENEERING

ABCM Brazilian Society of Mechanical Sciences and Engineering
27th ABCM International Congress of Mechanical Engineering
December 04-08, 2023, Florianópolis-SC, Brazil

COB-2023-0736
WEAR RESISTANCE EVALUATION OF THE COATING DIN 8555: MF 10-GF-60-GRZ ON THE HARDOX® 450 STEEL APPLIED IN THE RECOVERY OF MINING TRUCK BODY

Thais Stefany Santiago Brandão
Gilmar Cordeiro da Silva
PUC Minas – Graduate Program in Mechanical Engineering, Av. Dom José Gaspar, 500, 30.535-901, Belo Horizonte – MG, Brazil.
thaisfany1@hotmail.com
gilmarcord@gmail.com

Anderson Junior dos Santos
UFMG – Universidade Federal de Minas Gerais, Av. Pres. Antônio Carlos, 6627, 31.270-901, Belo Horizonte – MG, Brazil.
andersonsantos@cefetmg.br

Abstract. *In the mining industry, equipment deterioration due to abrasive wear can lead to reduced future revenue and to increase equipment availability, abrasion-resistant plates and linings are used. Hardox® steel is used in the manufacture of off-road truck weighbridges. With this in mind, this work proposed a study into the application of the hardfacing DIN 8555: MF 10-GF-60-GRZ in the areas with the highest incidence of wear on the truck body, as an alternative to protect the base metal to increase durability and, consequently, extend the lifespan of the equipment. The present study was intended to assess whether the material could be used to cover Hardox® 450 using the flux-cored arc welding (FCAW) process, in order to compare the performance of the plate with and without the covering in relation to abrasive wear. The methodology consisted of evaluating metallic properties, with chemical analysis, microstructure analysis, microhardness and a comparison of wear resistance using the pin-on-disk test. With the results obtained, it was possible to verify that the properties of the hardfacing were compatible with the base metal, so with its application it is possible to have good efficiency in the operation.*

Keywords: *Wear, Hardox® 450, Hardfacing, Welding, Pin-on-disk*

1. INTRODUCTION

In the contemporary 21st century, the world is constantly changing in all spheres of organizations, making the development of devices and equipment increasingly complex. This requires a thorough analysis of management, with the need to define goals and priorities so that equipment becomes more efficient and competitive. According to Oliveira (2020), the satisfactory availability of equipment suggests an organization's production capacity and, consequently, a reduction in costs and a guarantee of good product quality. As reported by IBRAM (Brazilian Mining Institute) in 2021, the mineral sector recorded a 62% increase in revenues compared to 2020, totaling R$ 339.1 billion (excluding oil and gas) and Brazilian mineral exports reached US$ 58 billion, an increase of 58.6% compared to 2020. The ore is processed through various industrial processes using state-of-the-art technology and then sold to the steel industry.

During ore extraction, the equipment used in the process deteriorates through abrasive wear of the area in contact with the mineral, due to the forces of impact and friction. The wear and tear of components and equipment in mining, as well as in other sectors of activity, has the effect of reducing future turnover, as it is an agent of capital depreciation, maintenance expenses, replacement of components and even the interruption of operations due to maintenance shutdowns. When it involves abrasive wear, the industry use abrasion-resistant plates and coatings to increase the availability of mining equipment (ILIN, et al., 2019).

The high abrasion-resistant steels used in plates and coatings have few alloy elements in low percentages in their chemical composition, with equivalent carbon in the order of 0.48 to 0.73, such as the Hardox® steels produced by Svenskt Stål Aktiebolag (SSAB) (ÖZTURAN et al, 2022). Gonçalves, P. (2021), says that off-road truck buckets are generally made from high-hardness steels, such as high-manganese alloy steels, high-chromium cast iron and tempered low-alloy steels, where these materials guarantee good performance under wear conditions.

Hardfacing weld metal overlay refers to weld deposits made, using a variety of processes, to prevent the effects of wear and/or abrasion (ASME IX, 2019). This deposition can be done using various techniques, depending on the type of wear and the thickness of the coating applied. A comparative analysis of various approaches to coating surfaces shows that flux-cored arc welding (FCAW) has significant advantages, such as production efficiency and control of the thickness of the coating layer (BEMBENEK, et al., 2022). The FCAW process has the advantage of being able to be applied to

localized areas of the part that are more subject to wear, which can extend the lifespan of sheets, both new and worn (SHIHAB, et al., 2020).

According to Costa, Vendramini and Ribeiro (2019), welding with tubular wire is a process in which the coalescence of metals is achieved by heating an arc between a continuous tubular electrode (which performs the functions of stabilizing the arc and adjusting the composition of the weld) and the material. This type of welding can be done with shielding gas or using self-shielded wire.

For this work, Hardox® 450 steel was chosen, manufactured by SSAB, by hot rolling and subjected to tempering heat treatment (LIGIER et al., 2022). It has a nominal hardness of 450 HBW and is supplied in thicknesses from 3.2 to 130 mm (SSAB, 2021). And for the hardfacing application, Ø 1.6 mm tubular wire was chosen, which meets the AWS DIN 8555/MF-10-GF-60-GR classification supplied by ESAB. In other words, wear resistance is achieved by increasing hardness, so when a truck body requires maintenance, all the wear plates are replaced, regardless of their condition.

In this context, this article proposes a study to apply hardfacing to the areas of highest incidence of wear on an off-road truck. This additional layer of material could be an alternative for protecting the base metal and recovering consumed parts to increase durability and, consequently, extend the lifespan of the equipment, in order to avoid having to stop to replace all the sheets.

2. PROCEDIMENTO EXPERIMENTAL

In this study, Hardox® 450 steel was used as the base metal, supplied in thick plate form and with a thickness of 12.7 mm, and for the hardfacing, Ø 1.6 mm tubular wire, which meets the AWS DIN 8555/MF-10-GF-60-G classification, is a high-carbon, high-chromium tubular wire, with no added carbide formers, which is abrasion-resistant and stainless.

The chemical compositions of Hardox® 450 and the weld metal are given in Table 1 and the mechanical properties of the materials are given in Table 2 based on the supplier's certificates.

Table 1. Chemical composition of Hardox® 450 and deposited weld metal (%).

Material	C	Si	Mn	P	S	Cr	Ni	Mo	B
Hardox® 450[(1)]	0,26	0,70	1,60	0,025	0,01	1,40	1,50	0,60	0,005
Weld metal [(2)]	4,00	0,77	0,082	0,006	0,026	21,74	-	-	-

[(1)] maximum values in (%)
[(2)] values found in the chemical analysis of the deposited metal in (%)

Table 2. Properties of Hardox® 450 and deposited weld metal.

Material	Hardox® 450	Weld metal
Tensile strength (MPa)	1412	590
Yield strength (MPa)	1250	550
Charpy-V (J) impact test	50	65
Temperature (°C)	-40	-30
Hardness (HRC)	44,5	60

The welding method was FCAW and was performed by a welder qualified according to the AWS for the procedure. The equipment used was a Miller Deltaweld 852 welding machine, a Minipa MT-350 digital infrared thermometer to check that the maximum welding interpass temperature was not exceeded, and a calibrated voltmeter and ammeter to guarantee the reliability of the welding parameters.

Due to the base sheet's thickness of 12.7 mm, it was not necessary to preheat it before starting the process, in accordance with the supplier's recommendations. The welding parameters were set according to the data provided by the consumable supplier, as shown in Table 3, and no shielding gas was used as the wire was self-protected. From the average welding voltage, current and speed values, it was possible to obtain the heat input used in the procedure.

Tabela 3. Parâmetros de solda.

Processo de soldagem	FCAW
Welding voltage (V)	24,2 a 25,4 V
Welding current (A)	183 a 195 A
Welding speed	160 a 165 mm/min
Heat efficiency	0,8
Heat input	1,3845 kJ/mm
Arame tubular	DIN 8555 MF-10-GF-60-GR

The sheet metal used to make the wear test specimens was fixed on a stand to perform the procedure. The surface of the sheet was prepared by grinding to remove oxides, grease and any other impurities.

During the flat welding process, the plate had two layers of material deposited on the entire surface in accordance with the guidelines received from the supplier in order to obtain the best results. The passes were performed with a maximum width of 10 mm and a maximum thickness of 3 mm per pass, as illustrated in Figure 1.

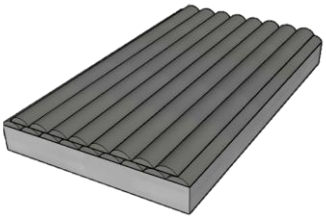

Figure 1. Coated sheet

After the welding procedure, the specimens were cut, milled and their surfaces ground to guarantee uniformity and to obtain an average roughness (Sa) of less than or equal to 0.8 μm in accordance with ASTM G99-04 for the wear test.

2.1 Chemical analysis

In order to certify the materials tested, the chemical compositions of the base material and the hardfacing were obtained through chemical analysis by spectrometry - iron base performed at the Materials Testing and Analysis Laboratory - LAMAT using the SPECTROMAXx optical emission spectrometer, with samples taken from the base sheet and the hardfacing sheet.

2.2 Microstructure and microhardness analysis

The base metal and coated base metal were subjected to microstructural and microhardness analysis. The coated base metal specimens were taken from the cross-section of the welded sheet, while the base metal specimens were taken from the base sheet. These specimens were prepared for microhardness and microstructure analysis using the following procedures: embedding, grinding to 1500 mesh, polishing with a 3-μm and 1-μm diamond suspension and chemical attack with 2% Nital for 10 seconds.

The microstructural analyses were performed using an Olympus optical microscope, Model: BX 51M, equipped with an image acquisition and processing system.

For microhardness, a Shimadzu microdurometer with magnification of up to 400X was used. The load used in the test, defined after the pre-test, was 980.7 mN (HV 0.1) and the time for each indentation was 15 seconds in accordance with ASTM E384-22. The distance between each indentation was 4x the diagonal measurement of the impression, which is the minimum recommended by the ASTM E384-22 standard.

2.3 Wear test

To determine wear resistance, pin-on-disk abrasive wear tests were performed in accordance with ASTM G99-04. A Microtest tribometer, specifically model SMT-A/0100, serial number B01100-19, of the pin-on-disk type, was used to determine the coefficient of friction (μ) of the specimens with and without coating. The measurements were taken using the Nanovea Tribometer Software program.

The test was performed without lubrication, with controlled air temperature and humidity of 20ºC ± 1 ºC and 50% ± 1.3%. The specimens and pins were cleaned with alcohol and dried to remove any impurities and particles.

The wear on the base metal and the coated base metal was determined by repeating 3 tests for each situation with the parameters in Table 4.

Table 4. Wear test parameters.

Test	Pin-on-Disk
Speed	240 rpm
Load	20 N
Distance	52 m
Track diameter	5 mm
Time	14 minutes

The spherical top pins used in the test were made from WC-Co metal-ceramic composite with ultra-fine grains in the range of 0.2 to 0.5 μm, with a diameter of 6 mm and a length of 15 mm. This material was chosen because hard metals are wear-resistant materials due to their hardness and toughness (KARIMI; HADI, 2020), which is beneficial for use in parts subjected to work with iron ore, as they are abrasive and hard, as is the case with off-road trucks in the mining industry.

The pin-on-disk test results in wear on both the pin and the specimen (S) with the formation of a wear track. After the test, the wear tracks were measured and analyzed in 3 different regions by profilometry using the HommelwerkT8000 profilometer and the Hommelmap Expert 6 analysis software. The width of the tracks was obtained from this measurement and the average and standard deviation of the volume of material removed from the specimens were calculated. According to the ASTM-G99 standard, when only the specimen has significant wear, the volumetric loss of the specimen can be determined using Eq. 1.

$$Q = \frac{\pi * r_t * (b_t)^3}{6 * r_p}, \quad (1)$$

where Q= volumetric loss [mm^3], r_t= radius of the wear track [mm], b_t= width of the wear track [mm] and r_p= radius of the spherical top pin.

The specimen wear rate, known as the k coefficient, was calculated according to Archard's Law, as shown in Eq. 2, as a function of the volumetric loss, the load applied, and the distance covered.

$$k = \frac{Q}{W * D}, \quad (2)$$

where k= wear coefficient [$\frac{mm^3}{m*N}$], Q= volumetric loss [mm^3], W= normal test load [N] D= distance covered [m].

The comparison between the wear rates of the base metal and the coating was made possible by analyzing the value of the k coefficient (HUTCHINGS and SHIPWAY, 2017).

3. RESULTS

3.1 Chemical analysis

The concentrations of the chemical elements present in the base metal in percentage by weight are shown in Table 5. Comparing the results obtained with the SSAB supplier's analysis in Table 2, it can be seen that the concentration of all the chemical elements present in the base metal varies, in smaller quantities, from the supplier, because the values in the specification refer to the maximum limits.

Table 5. Chemical composition of Hardox® 450

C	Si	Mn	P	S	Cr	Ni	Mo	B
0,154	0,256	1,246	0,018	0,003	0,079	<0,0225	<0,0045	0,0012

The percentage of chromium found is approximately 15 times lower than the maximum limit of 1.40%. Nickel and molybdenum, whose maximum limits are 1.50% and 0.60% respectively, were found in quantities of less than 0.1%. It is believed that due to the high cost of nickel and molybdenum nowadays, the reduction in manufacturing costs may have involved a reduction in alloy elements. To offset these reductions, it is considered that the use of boron may have been chosen, which in this case would improve the strength and toughness of the material (SILVA, et al, 2022).

In another point, although not listed explicitly in the chemical composition provided by the supplier, the presence of aluminum was detected, with a concentration of 0.029%, titanium, with a concentration of 0.02%, copper, with a concentration of 0.015%, and niobium, with a concentration of 0.014%. In this case, the aluminum in the material has the function of reacting with nitrogen, which is found in a concentration of less than 0.0029%, while the titanium has the function of fixing nitrogen.

In the weld metal, the concentrations of the chemical elements present in percentage by weight are shown in Table 6, and the results are in accordance with the supplier’s information in Table 2.

Table 6. Chemical composition of the weld metal

C	Si	Mn	P	S	Cr
3,617	0,862	0,912	0,010	0,008	19,28

The chromium in higher percentage is added to improve the properties of resistance to corrosion and oxidation and the carbon is contributed to harden it and improve its mechanical properties, it forms carbides with the chromium in the alloy, contributing to strength and hardness.

3.2 Microstructure and microhardness analysis

Micrography analysis was performed at 50x and 100x magnification of the Hardox® 450 (0.154% by weight C) and at 20x and 50x magnification of the HAZ. The microstructure of the Hardox® 450 base metal is presented in Figure 2. The non-uniformity of the structures, with dark and light areas, indicates that the microstructure of the material is mainly composed of a martensitic matrix with a dark color, which is formed due to fast cooling during hardening. The lighter areas probably consist of carbides and retained austenite.

The microstructure of the Hardox® 450 HAZ is illustrated in Figure 3 and is made up of pearlite and ferrite grains. During the cooling of the austenitic phase formed as a result of the heat in the welding process, these grains nucleated in different directions in the inclusions of the material. The ferrite and pearlite phases can be differentiated after 2% Nital attack, where the pearlite is found in the dark regions. This microstructure was also observed by Özturan, et al. (2022) when analyzing the HAZ of Hardox® 450 in a welded joint.

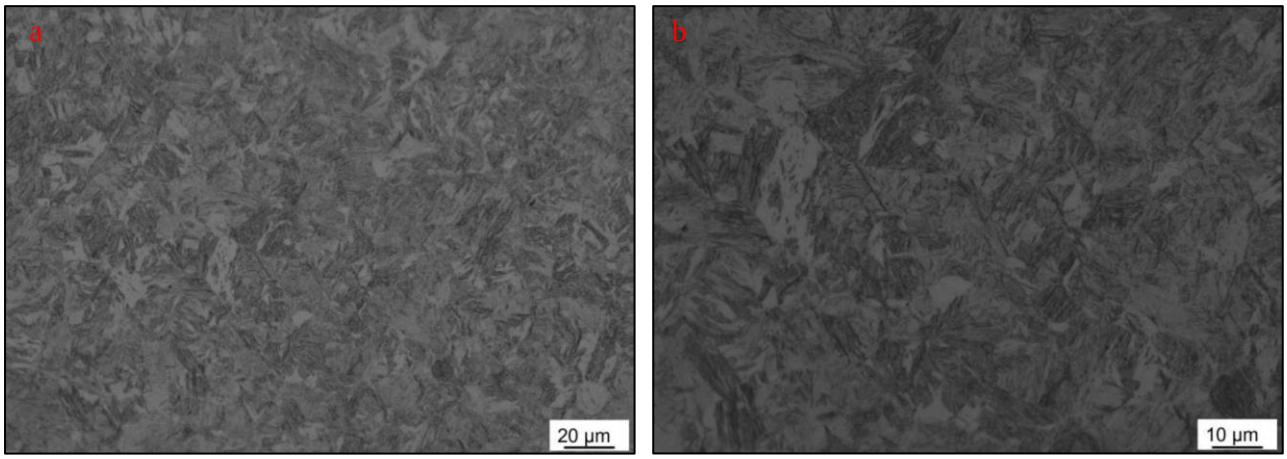

Figure 2 - Base metal microstructure a) 50x and b) 100x

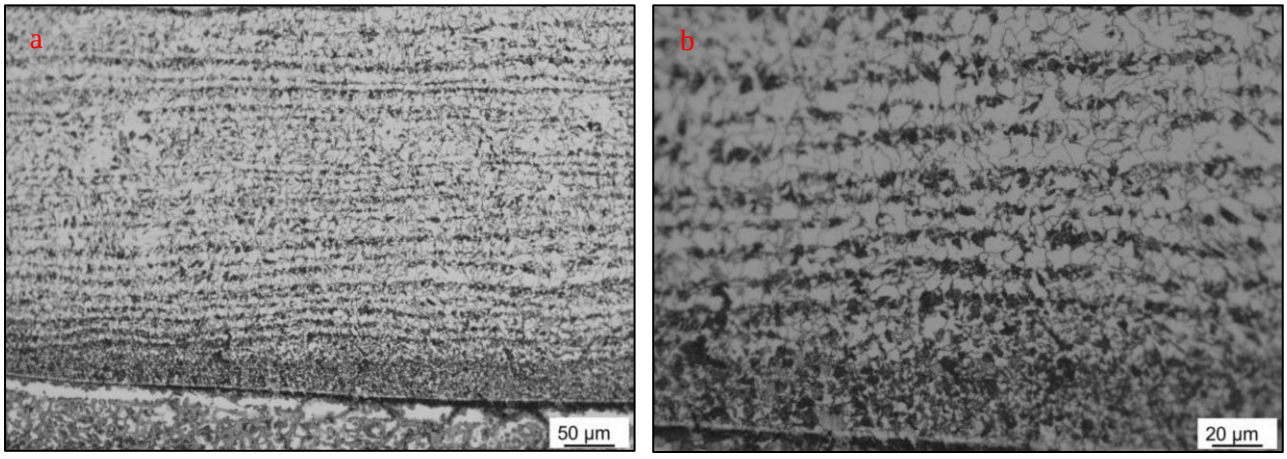

Figure 3 - HAZ microstructure of the base metal a) 20x and b) 50x

The coating with (3.617% by weight C) has its microstructure represented in Figure 4 and is made up of an austenitic matrix, secondary carbides and pearlite grains. It can be seen that the coating showed a microstructure consisting of austenite in a eutectic matrix, in which austenite coexists with carbides, forming a layer composed mainly of primary hexagonal carbides (M_7C_3). This microstructure was also observed in the studies by Oliveira and Costa (2019) and also by Souza and Ferraresi (2017) with the application of FeCrC coatings.

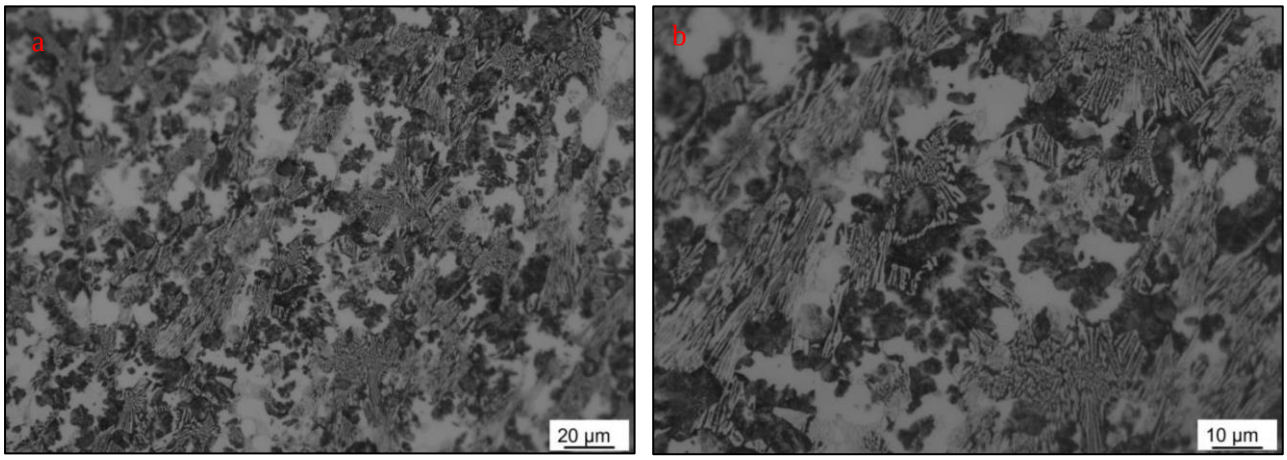

Figure 4 - Coating microstructure a) 50x and b) 100x

For the microhardness tests, a load of 980.7 mN (HV 0.1) was used with a time of 15s for each indentation. After 10 measurements of each material, the average microhardness values for Hardox® 450 was 490.5 HV, the HAZ of Hardox® 450 was 200.5 HV and the coating was 739.8 HV according to Table 7.

Table 7. Microhardness (HV) of Hardox® 450, Hardox® 450 HAZ and coating

Test	Hardox® 450	Hardox® 450 HAZ	Coating
1	470	206	770
2	484	201	780
3	522	198	743
4	512	200	743
5	493	198	752
6	475	188	752
7	479	214	789
8	493	201	743
9	493	202	770
10	484	197	770
Average	**490,5**	**200,5**	**761,20**
Standard deviation	**15,33**	**6,30**	**15,88**

Among the various microstructures that can be obtained in an alloy steel, martensite stands out for being the hardest and most resistant, although it is also the most fragile. It is believed that the strength and hardness of martensite do not depend directly on its microstructure, but rather on the ability of interstitial carbon atoms to restrict the movement of discordances, as well as the reduced amounts of slip systems present in the TCC (Tetragonal Centered Body) structure (CALLISTER, 2016).

The Hardox® 450 HAZ showed a significant reduction in microhardness; this reduction was also found in other studies after welding; according to Viegas (2016), the specimens that received hardfacing welds had a drop of around 48% in the Vickers microhardness value, measured along the thickness of the base metal. Similarly, the results of Özturan et al (2022) showed an average hardness value of 468 HV in Hardox® 450 steel. However, in welded specimens, a considerable decrease in hardness was noted, reaching around 240 HV in the HAZ.

The microhardness measured in the weld metal is in accordance with that provided by the supplier ESAB, which varies in the range 57< HRC ≤ 62, where the microhardness found is in the range 62 HRC.

3.3 Wear test

The assessment of wear in the tests was performed by analyzing the amount of material lost by the specimen in relation to the distance covered during the pin-on-disk test. Table 8 shows the profilometry results of the wear tracks of Hardox® 450 without and with coating. The values shown reflect the average and standard deviation of the width and

depth of the wear tracks of three regions identified after the profilometry analysis. The average track width values found were applied to Eq. 1.

Table 8. Profilometry analysis of the wear tracks

	Measurement	Track width (mm)	Track depth (mm)	Track area (mm^2)
Hardox® 450 without coating	1	0,3600	0,0042	0,0019
	2	0,3750	0,0063	0,0032
	3	0,3700	0,0050	0,0023
	Average	**0,3683**	**0,0052**	**0,0024**
	Standard deviation	**0,008**	**0,0010**	**0,0007**
Hardox® 450 with coating	1	0,2650	0,0009	0,00049
	2	0,2850	0,0010	0,00046
	3	0,2690	0,0009	0,00048
	Average	**0,2730**	**0,0009**	**0,0005**
	Standard deviation	**0,0106**	**0,0001**	**0,00001**

The profilometry analysis indicates a 35% reduction in track width with the coated material, and a 478% reduction in track depth compared to the base material. With these values, it is evident that the application of the coating resulted in a reduction in wear. This can be confirmed by the area of the track, which was also reduced by 380%. This reduction in track wear is shown in Figure 6a and 6b.

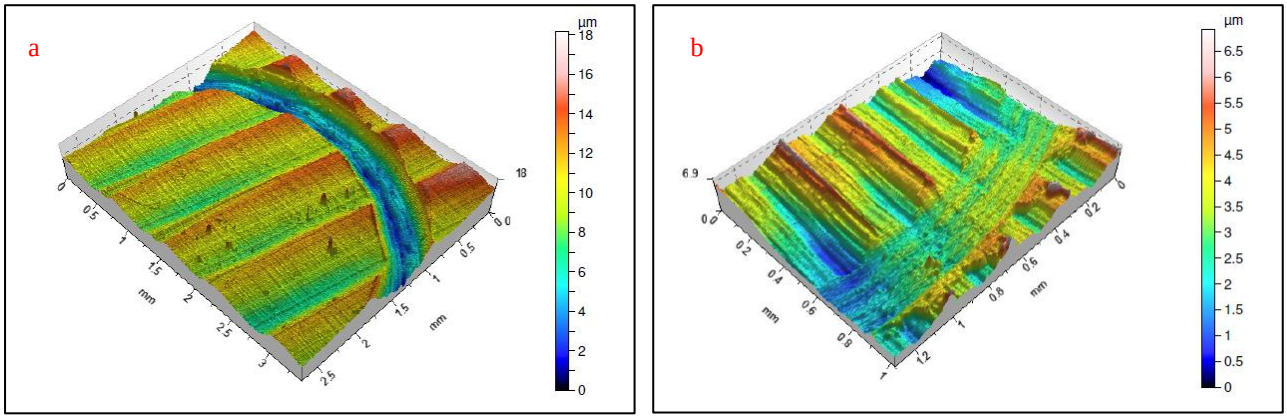

Figure 6 Hardox® 450 wear tracks a) without coating and b) with coating.

In Table 8, the volumetric loss and wear rate values are calculated using Eq. 1 and 2 for Hardox® 450 and the coating. It can be seen that the volume lost, and the wear rate were lower for the coating, which supports the average value found for the track depth for this circumstance.

Table 8. Volumetric loss and wear rate values for Hardox® 450

	Without coating	With coating
Load - W (N)	20	20
Distance (m)	52,0	51,8
Average track width (mm)	0,3683 ± 0,008	0,2730 ± 0,0106
Volumetric loss - Q (mm^3)	$2{,}18*10^{-2} \pm 1{,}10*10^{-3}$	$8{,}90*10^{-3} \pm 1{,}05*10^{-3}$
Wear coefficient - k ($mm^3/m * N$)	$2{,}10*10^{-5} \pm 1{,}06*10^{-6}$	$8{,}56*10^{-6} \pm 1{,}01*10^{-6}$

In Figure 7 is the evolution of the friction coefficient curves (μ) up to a time of 14 minutes. The average μ values were taken when the curves reached the stationary stage. It was found that the behavior of the μ curves for the Hardox® 450 without coating was similar, however due to the difference in the behavior of the μ curve between the S1 and S2

conditions, the third test was necessary. In relation to the μ curves for Hardox® 450 with coating of S's 4, 5 and 6, we observed similar curves with more stability compared to S's 1, 2 and 3. This suggests that the stationary stage was reached after 5 minutes and the μ values were relatively constant.

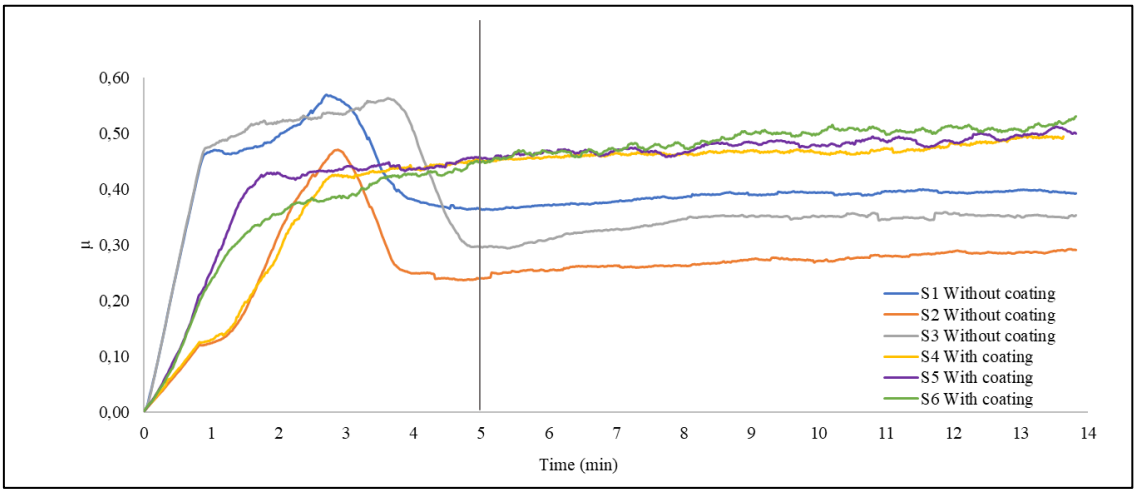

Figure 7. Coefficient of friction during the test period.

The variations observed can be attributed to the presence of debris, which causes instability in the friction coefficient curve due to the deformation and breaking of the asperities, because during the initial phase (run-in), the surfaces in contact are adjusting. After this, the debris is removed from the surface and a real contact area is formed, resulting in the stabilization of friction (Ba et al., 2021). Table 9 shows the μ values for Hardox® 450 without coating and with coating from the stationary stage.

Table 9. Friction coefficient values (μ).

Hardox® 450	Friction coefficient (μ)
Without coating (S's 1, 2 e 3)	0,33 ± 0,06
With coating (S's 4, 5 e 6)	0,48 ± 0,01

Although the friction curves are statistically different, the average values are similar, indicating that the variations in hardness between Hardox® 450 and the coating did not have a substantial impact on the friction coefficients over the test period.

4. CONCLUSION

When comparing the properties of Hardox® 450 and the coating applied, the following results were obtained:

Resistance to abrasive wear was higher for the coating, where volumetric loss (Q) and the wear coefficient (k) showed values 145% lower compared to the base material. This improvement may be related to hardness, where the coating had a 55% increase compared to Hardox® 450. Harder materials are generally more resistant to abrasion, so the penetration of particles into the surface of the material is lower and consequently wear is reduced.

The influence of hardness levels in the base metal and coating is hardly notable in the coefficient of friction values, as they remained consistently within the μ = 0.2 to μ = 0.6 range, with averages varying between 0.33 and 0.48.

The results indicate that the coating in question can be considered a good material to be applied to the repairs of truck body in the field, being applied to the wear areas, avoiding a longer shutdown time for the complete replacement of the sheets, prolonging the lifespan and productivity of the equipment.

Considering a truck with a payload of 258.40 tons, an average loading and unloading cycle time of 13 minutes and a productive hour of 50 minutes due to inefficiencies in the process, there are 3.85 trips per hour. Applying the 83% efficiency to the hourly productivity, we have a load of approximately 825 tons/hour of ore. With this, when analyzing the average price of a ton of iron ore (January to September/23), we have a value of US$ 116.95, and if we consider 1 hour of the truck shutdown for maintenance, we have a loss of approximately US$ 96 K.

5. ACKNOWLEDGEMENTS

To DELP Mechanical Engineering and all its staff, especially my father who supported me with his knowledge, experience, materials, labor and all the necessary resources.

To PUC/Minas and the support of the Coordination for the Improvement of Higher Education Personnel (CAPES) - funding code 001.

6. REFERENCES

ASME, 2019, *American Society of Mechanical Engineers*. ASME IX BPVC IX: Welding, Brazing and Fusing Qualifications.

ASTM, 2017, *American Society for Testing and Materials*. G99-04: Standard Test Method for Wear Testing with a Pin-on-Disk Apparatus.

ASTM, 2022, *American Society for Testing and Materials*. E384-22: Standard Test Method for Microindentation Hardness of Materials.

BA, Elhadji Cheikh Talibouya *et al*., 2021, Investigation of the effects of skewness R_{sk} and kurtosis R_{ku} on tribological behavior in a pin-on-disc test of surfaces machined by conventional milling and turning processes. Materials Research, v. 24, p. e20200435.

Bembenek, Michał *et al*., 2022, "Microstructure and Wear Characterization of the Fe-Mo-BC—Based Hardfacing Alloys Deposited by Flux-Cored Arc Welding". *Materials*, v. 15, n. 14, p. 5074.

Callister, Willian D; Rethwisch, David G., 2016, *Ciência e engenharia de materiais: uma introdução*. 9. Ed. Rio de Janeiro: LTC.

Costa, A. F.; Vendramini, J. R.; ribeiro, V. M., 2019, "Análise de desgaste dos revestimentos por soldagem para recuperação das guias do carro alimentador da caixa matriz fabricadas em aço SAE 1045". *Revista Vincci - Periódico Científico do UniSATC, [S. l.]*, v. 4, n. 2, p. 149–178.

IBRAM. *Inforgráfico Mineração em números*. 2021. Disponível em:< https://ibram.org.br/>. Acesso em: 29 julho 2022.

Ilin, S.; Adorska, L.; Samusia, V.; Kolosov, D.; Ilina, I., 2019, "Conceptual bases of intensification of mining operations in mines of Ukraine based on monitoring and condition management of mine hoisting systems". *E3S Web Conf*., 109, 00030.

KARIMI, Hadi; HADI, Morteza., 2020, "Effect of sintering techniques on the structure and dry sliding wear behavior of WC-FeAl composite". *Ceramics International*, v. 46, n. 11, p. 18487-18497.

Gonçalves, Paulo César, 2021. *Manuseio de minério de ferro coesivo sob umidade natural*. Dissertação (Mestrado em Engenharia Ambiental) - Escola de Minas da Universidade Federal de Ouro Preto, Ouro Preto, Brasil.

Hutchings, Ian; Shipway, Philip., 2017, *Tribology: friction and wear of engineering materials*. Butterworth-Heinemann.

Ligier, K., *et al*., 2022, "Analysis of Wear Properties of Hardox Steels in Different Soil Conditions". *Materials*, v. 15, n. 21, p. 7622.

Oliveira, Tatiane Gabi de, Costa, Adilson Rodrigues da., 2019, "Influência da microestrutura na resistência ao desgaste microabrasivo de ligas de F-Cr-C e Fe-Cr-C-Nb". *Revista Materia (Rio de Janeiro)*, v.24, n. 01.

Oliveira, Otávio J., 2020, *Gestão da qualidade: tópicos avançados*. Cengage Learning.

Özturan, A., *et al.*, 2022, "Study of the microstructure and mechanical property relationships of gas metal arc welded dissimilar Hardox 450 and S355J2C+N steel joints". *Materials Science and Engineering: A*, v. 856.

Silva, Abílio P. *et al*., 2022, "Hardox 450 Weld in Microstructural and Mechanical Approaches after Welding at Micro-Jet Cooling". *Materials*, v. 15, n. 20, p. 7118.

Shihab, Thaer *et al.*, 2020, "Thermodynamic Approach to the Development and Selection of Hardfacing Materials in Energy Industry". *Management Systems in Production Engineering*, v. 28, n. 2, p. 84-89.

Souza, Daniel Dominices Baía Gomes de; Ferraresi, Valtair Antonio., 2017, "Aplicação de revestimento duro utilizando o processo FCAW duplo arame para diferentes tipos de consumíveis utilizados na indústria sucroalcooleira". *Matéria (Rio de Janeiro)*, v. 22.

SSAB. *Data sheet 168uk Hardox 450*. 2021. Disponível em: <http://www.ssab.com>. Acesso em: 1 dez. 2022.

Viegas, Daniel Bicalho., 2016, "Avaliação da resistência ao desgaste de um aço Hardox® 450 submetido a solda de revestimento duro". In: 71º *Congresso Anual da ABM*. Rio de Janeiro.

7. RESPONSIBILITY NOTICE

The author(s) is (are) the only responsible for the printed material included in this paper.